2014 Canada-China Conference on Advanced Reactor Development (CCCARD-2014)
Niagara Falls Marriott Fallsview Hotel & Spa, Niagara Falls, Ontario Canada, April 27-30, 2014.

CCCARD2014-044

EXPERIMENTAL THERMAL-HYDRAULIC ANALYSIS OF A SUPERCRITICAL CO_2 NATURAL CIRCULATION LOOP

J. Mahmoudi[1], V. Chatoorgoon[1], R. W. Derksen[1] and L. Leung[2]
[1] University of Manitoba, Manitoba, Canada
[2] Atomic Energy of Canada Limited, Chalk River, Ontario, Canada

Abstract

Experimental thermal-hydraulic studies of a rectangular supercritical CO_2 natural circulation loop with a horizontal heated channel were conducted at different steady-state conditions. These included three different system pressures and three different inlet temperatures, with different inlet and outlet valve openings. Detailed information of friction-factor and local head loss coefficients were produced. Comparison shows that for the available experimental set-up, computed frictional pressure-drops fall within 1-1.2 of the Blasius formula. Moreover, flow oscillations were observed frequently when the CO_2 outlet temperature was higher than the pseudo-critical temperature on the negative slope part of the mass flow-rate versus power curve.

Introduction

The Super-Critical Water Reactor (SCWR) is one of the advanced designs for the new Generation IV reactors, which operates at super-critical pressures (25 MPa) on the primary side. A SCWR offers higher thermal efficiency for the plant and eliminates the need for recirculation and jet pumps, pressuriser, steam generators, steam separators and dryers. Similar to the Boiling Water Reactors (BWRs), there is a large variation in the density when the coolant is heated along the core of a SCWR. In addition to the density, all other thermo-physical and transport properties of the coolant change significantly near the pseudo-critical temperature at super-critical pressures. These changes may result in an undesirable phenomenon called Density Wave Oscillations (DWO). DWO is one type of thermal-hydraulic instabilities in which the velocity of the coolant at the inlet to the fuel bundle oscillates over time. These oscillations have to be avoided since they may induce vibration in the system or can burn-out the fuel bundle in a real case.

Natural circulation in BWRs is a proven technology that was employed in the Dodewaard (183 MWth) and Humboldt Bay (165 MWth) nuclear reactors. Economic Simplified Boiling Water Reactor (ESBWR) is the newest design of Generation III+ reactors that is solely operating based on the natural circulation principle to remove the reactor core heat without using a circulation pump in the system. Natural circulation is a passive safety feature that creates increased design safety, integrity, and reliability, while simultaneously reduces the overall cost of a reactor. Natural circulation could be employed as a design criterion for SCWRs similar to ESBWRs. Also, it could be employed as a back-up in SCWRs to remove reactor core heat in case of losing power to the circulation pump.

CO_2, Helium, or Freons are surrogate fluids that can be utilized for performing experiments in SCWR's research and development programs since they have considerably lower critical pressure and temperature. Therefore, their use will lead to significant time and cost reduction in constructing and operating the experimental facilities. The thermodynamic critical point of water is 374 ºC and 22.1 MPa, while it is 31.1ºC and 7.39 MPa for CO2. In the present study, CO_2 was used as the working fluid in a rectangular natural circulation loop.

Information from the steady-state operation of a Supercritical Natural Circulation Loop (SCNCL) could be used in numerical codes for studying flow instability. This information includes friction-factor correlation for the heated tube, inlet and outlet valve head loss coefficients, power, system pressure, and inlet temperature to the heated channel. Pressure drop is an important parameter in defining flow-rate and instability boundaries in a natural circulation loop.

Plenty of numerical analyses have been done on flow instability for super-critical flow, but there are very few experimental studies. These experimental studies did not provide all details of their tests to make them useful for validation of numerical codes.

Chatoorgoon [1] developed a one-dimensional stability numerical model (SPORTS Code) for supercritical flow in a single channel natural circulation loop. Also, a simplified theoretical criterion was introduced to verify the numerical prediction of flow instability boundary. Moreover, Chatoorgoon et al. [2,3] reported comprehensive numerical and analytical instability studies for different inlet pressure and temperature conditions with different inlet and outlet K factors, using different supercritical fluids (CO_2 and water) in natural circulation loops. They showed in their study that the onset of flow instability is within 95-100% of the maximum flow-rate in the mass flow-rate versus power curve. Jain and Uddin [4] carried out a numerical investigation for a SCNCL with CO_2 as the working fluid. They solved the one dimensional conservation of mass, momentum and energy equations using finite difference methods. Their results predicted the onset of instability somewhere in the positive slop region of steady state power vs. flow-rate curve.

Jain and Corradini [5] performed both numerical and experimental studies for a rectangular CO_2 natural circulation loop. They used both non-linear and linear approaches in their numerical simulation. Their simulations showed the inception of instability is in the negative slope portion of the flow-rate versus power curve at high powers. However, they didn't observe any clear evidence of flow instabilities in their experiment. They concluded that the occurrence of instability is dependent to the geometry, degree of sub-cooling, and operating power. Another experimental study has been reported by Lomperski et al. [6] at Argonne laboratory for supercritical CO_2 natural circulation loop. Their one-dimensional nonlinear numerical simulation showed flow oscillations, but they did not observe any evidence of instability.

Sharma et al. [7] reported experimental results of instability for supercritical CO_2 natural circulation loop with a horizontal heated channel and horizontal cooler. In addition to the horizontal heating and horizontal cooling configuration, they tried vertical heating and cooling, but they did not observe flow oscillations in those cases. They performed their experiments at pressures of 8.1-9.1 MPa with constant cooling water flow-rates in the

secondary side (10-15 lpm and 34 lpm) while they were increasing power on the heated channel. They did not have a flow-meter in their loop and therefore they were using the energy balance across the heated channel to calculate the mass flow-rate. When flow oscillations were observed the heater inlet temperature was between 27-31 ºC (close to the critical temperature) and the outlet temperature was oscillating between 29-45 ºC. They modified the NOLSTA code to include the wall heat capacitance effect and they showed that wall thickness stabilizes the system.

Chen et al. [8] reported flow instabilities in their supercritical water natural circulation loop. The oscillations were observed when the outlet temperature of water in the heated channel was close to the pseudo-critical temperature. The heated section in their study was placed vertically and an annular heat exchanger was placed horizontally at the top tier. In their experiments, power was increased gradually, and power, inlet and outlet temperatures, and wall temperature were recorded. Mass flow rate in their study was calculated using the energy balance. Experiments using three test-sections with different diameters were performed and they claimed observing both static and oscillatory types of instability. In their study, static instability was characterized by a sharp reduction in the mass flow rate when the outlet temperature of the heated channel was close to or higher than the pseudo-critical temperature. They recognized local fluctuations of the heated wall temperature as the dynamic instability.

Lv et al. [9] performed an experimental study for a supercritical water loop with a single vertical heated channel. Their study showed flow oscillations in the positive slope part of the mass flow rate versus power curve. The oscillations vanished by increasing the power level and they did not reach to the maximum flow rate (the peak mass flow-rate versus power curve) in their tests.

From this literature review it can be found that very limited experimental data is available for instability in supercritical natural circulation loops. Moreover, in many experiments, steady-state parameters of the loop were not addressed thoroughly to be useful in the numerical modelling and validation of licensed codes. It should be noted that, in all of the experiments reviewed in this section, flow oscillations were observed when the outlet temperature was close to the pseudo-critical temperature and no flow oscillations is reported at relatively high outlet temperatures (above the pseudo-critical temperature). Due to the lack of experimental studies on thermo-hydraulic analysis for SCNC loops and the importance of the prediction of flow instability, a SCNCL was built at the University of Manitoba to investigate the stability margins and to study pressure drop for flow of super-critical CO_2 in a horizontal heated tube. However, the first step toward studying flow instability is specifying steady-state information of a SCNCL. Therefore, it is necessary to provide detailed information of the experiment for each test in the steady-state conditions. The objectives of our study were to:

1- Procure a data bank of pressure-drop measurements along the heated channel

2- Provide detailed information of the loop parameters in the steady-state conditions. This information will be useful in numerical modelling of the experiments

3- Extend the available experimental results on flow oscillations for supercritical natural circulation loops

1. SCNCL Apparatus and Test Procedure

The experimental set-up is a rectangular loop with a horizontal length of 725.8 cm and a height of 101.6 cm, oriented vertically with the test section at the middle of the horizontal lower tier and a heat exchanger at the middle of the horizontal upper tier (see Figure 1). An accumulator (SB 600-10 A 1/002 S1 – 345 C) is connected to the cold side of the loop, with the aim of adjusting the pressure in the loop during experiments. Two pneumatic ball valves are located upstream and downstream of the heated channel to introduce pressure-drops in the system. An evacuation pump is attached to the right-side vertical leg of the loop for removing air from the loop. CO_2 grade 4.5 (99.995% purity) is used as the working fluid. Direct current electricity is passed through the Inconel tube in the test section for generating heat. A heating tape is wrapped around the right vertical leg to decrease the density of CO_2 in that leg and to initiate the flow in the loop. Supercritical CO_2 flows counter clock-wise in the loop. There is also a large settling chamber in the lower part of the loop which was not used in any of the experiments in the present study. The settling chamber can be part of the loop by closing or opening the manual ball valves (BV-1, BV-2, BV-3, and BV4). Figure 1 shows the schematic of the experimental loop used in this study. Also, Figure A1 and Table A2 in the Appendix show the loop dimensions and local pressure drop coefficients for area changes and elbows.

In addition to the mechanical components explained above, Figure 1 shows the measured data during each experiment. An absolute pressure transducer is connected to the loop, below the accumulator, to measure the system pressure. Two resistance temperature detectors (RTDs) are connected to the inlet and outlet of the heated channel for measuring the flow temperature. It should be noted that there is no mixing chamber at the outlet of the heated channel and therefore, RTD2 is not a representative of the mass flow averaged temperature. RTD2 is not used in any calculation in this study. There are also four 1/8” K-type thermocouples for measuring the temperature at the inlet and outlet of the heat exchanger in the CO_2 side and in the water side (Cooling loop). There are also twelve 1/16” K-type thermocouples attached to the bottom and top of the heated channel surface at six locations along it for measuring the wall surface temperature. Nine differential pressure transmitters are located at different parts of the loop to measure the pressure drop. Pressure drop across the inlet and outlet pneumatic valves, total and the segmental pressure-drops along the heated channel, and pressure drop across the heat exchanger in the CO_2 side are measured. Voltage-drop across the heated channel and amperage from the rectifier are measured for calculating the applied heat on the channel. Volumetric flow rate of the CO_2 in the loop is measured by using a turbine flow-meter. Also a paddlewheel flow meter is used to measure the cooling water flow-rate.

The heated channel is a 259 cm long Inconel 625 polished circular pipe (OD: 0.75”, ID: 0.51”) which is heated by DC current through two conductors welded to the flanges (1” Class 2500, WN XXS) on either side of the heated channel. Inconel 625 has good electrical and thermal conducting properties which provide uniform heat flux on the heated tube. Two pieces of 1/8” coupling are welded to 1” (SCH. XXS) for measuring the flow temperature and pressure-drop. It should be noted that the heated section is 278 cm considering the distance between inlet and outlet taps for measuring the total pressure drops along the channel. The loop has been insulated with fiberglass insulation. Lab-View was used for monitoring and recording data. In Lab-View, the sampling rate of reported results was 0.01s for the DP cells and 1s for the thermocouples and RTDs.

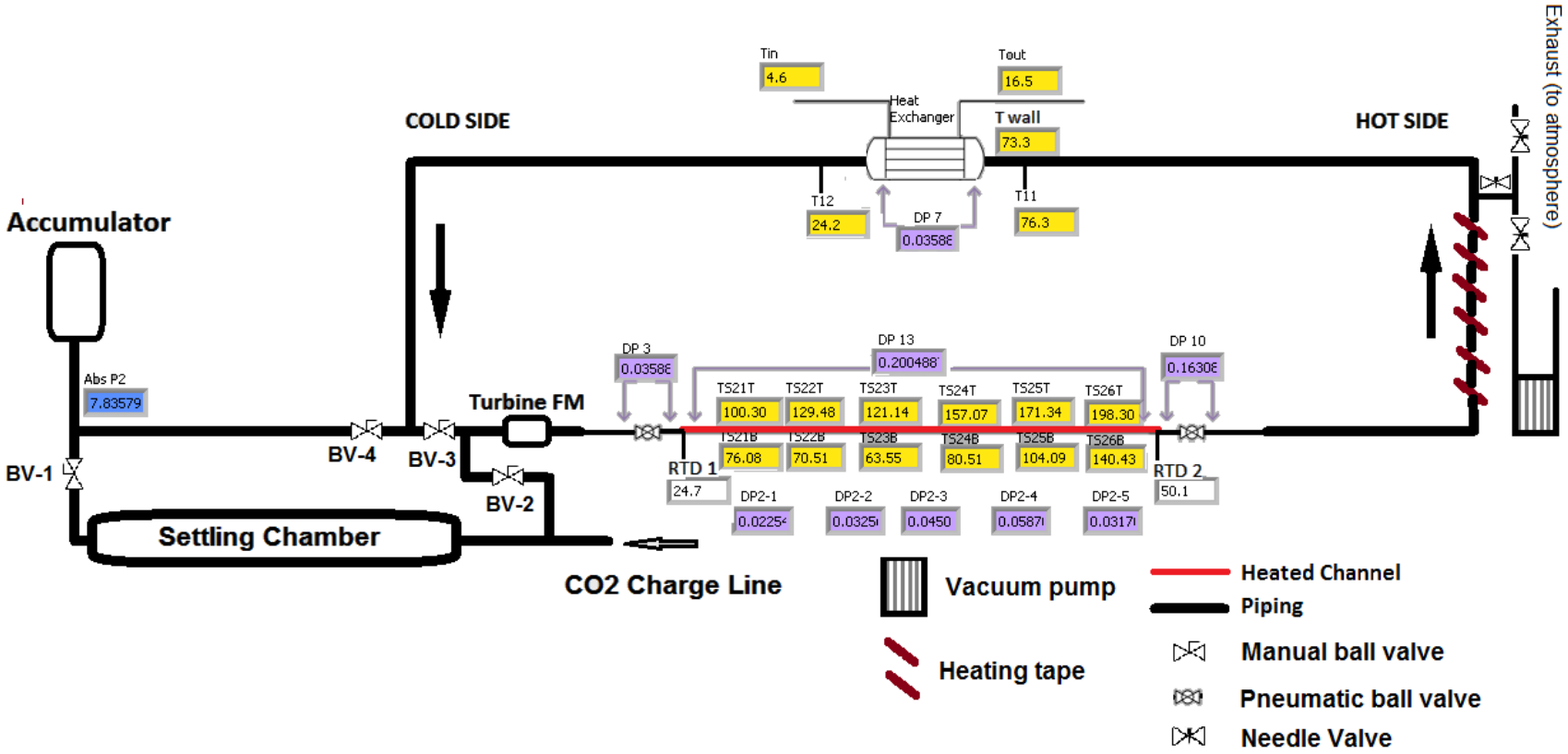

Figure 1 Schematic of the supercritical natural circulation loop

The very first step in each set of runs which include multiple data sets is calibrating the DP cells and doing the leakage test for all fittings and connections as a time consuming and demanding task. After eliminating all leakages, the evacuation pump is used to evacuate the loop for twenty four hours. This step is important to make sure that there is no air in the loop. Afterward, a booster pump is used to pressurize the loop. To initiate the flow in the natural circulation loop a heating tape which is installed on the right hand side riser is turned on. After a while, by opening up the cooling water supply in the secondary side, circulation of CO_2 in the primary side is initiated.

By heating the test section, both the flow-rate and pressure of the loop are increased to the desired working conditions. Meanwhile, the regulating valve on the accumulator is set to higher pressures to help in pressurizing the loop. Proceeding in this condition with putting more heat compare to removed heat from the heat exchanger leads to heating up the loop. To introduce the desired pressure-drop at different parts of the loop, pneumatic valves are used. This is done easily by adjusting the desired angle for the ball valve. During each set of experiments for steady-state conditions (each experimental curve of the flow-rate versus power) all pneumatic valves remain untouched after the initial adjustment, for the entire period of the experiment. After a while the desired working pressure and temperature at the inlet of the heated channel attained at specified valves opening position.

Then data taking is started for about five minutes for each steady-state run. The power increment is 0.7-0.8 kW in each step and transient time for getting to a new steady-state condition varies from half an hour up to one hour.

In a natural circulation loop, flow rate is dependent to the power on the heated channel, pressure-drop, inlet temperature, and system pressure. Test matrices were developed based on these independent variables and experiments were performed.

2. Experimental Results

The experimental investigations reported in the present study include frictional pressure-drop comparison, loop parameter in the stead-state conditions, and one case of flow oscillations. The comprehensive study was done by Mahmoudi [10] for 32 “data set” with different operating conditions (inlet temperature, system pressure, and valves position) for the loop. Experiments were performed at different pressures of 7.6, 8, 8.5, and 9.5 MPa and three different inlet temperatures of 20, 25, and 30 ºC, with different inlet and outlet valve openings. For each “data set”, inlet temperature to the heated channel, system pressure, and valves position were kept constant and power was increased as a step function. Power was increased for each data set this way till one of the limiting parameters (maximum power coming from the rectifier, cooling capacity of the secondary side, or heated wall surface temperature at TS25B) was reached. Each “data set” consists of several steady-states “data points” which were obtained within 7-8 hours of continues operation of the loop in one day. Approximately, 450 steady-state data points were collected and analysed (two data sets were repeated for the purpose of repeatability). For each steady-state data point, pressure-drop along the heated channel, flow-rate, power, flow and heated wall surface temperature were recorded. Propagation of uncertainties was calculated based on the numerical method outlined by Moffat [11].

2.1 Pressure Drop

The methodology used for deriving frictional pressure-drop is based on the survey conducted by Pioro et al. [12] on hydraulic resistance of the supercritical fluids flowing in heated channels. Figure 2 shows the variation of pressure-drop components along the channel for a data set. By increasing power, outlet density decreases and acceleration pressure-drop increases. Calculated acceleration pressure-drop was deduced from measured channel pressure drop and the frictional pressure-drop was obtained. Figure 2 shows that at large values of q/G the acceleration pressure-drop becomes significant, however at lower q/G frictional pressure drop is larger.

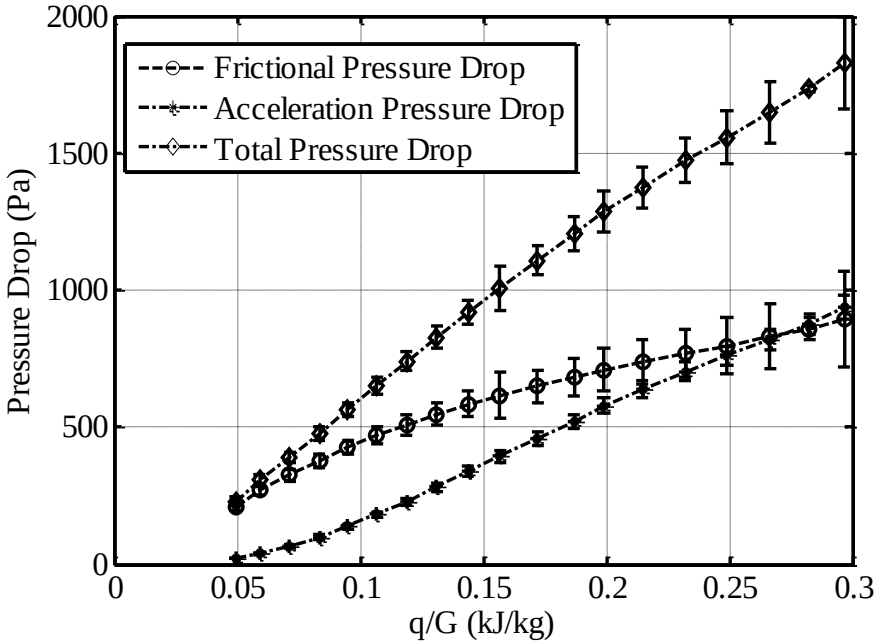

Figure 2 Variation of pressure drop components across the horizontal heated channel in a natural circulation loop for a data set

The results of comparison of frictional pressure-drop from available correlations (Appendix: Table A1) and frictional pressure-drop from experiment are shown in Figure 3 for one data set. This figure shows that the frictional pressure-drop for this data set is slightly higher than the pressure-drop calculated based on available friction-factor formulas for supercritical flow, except for the data of Kuraeva and Protopopov [13]. Although Kuraeva and Protopopov were the only ones who included the effect of buoyancy (Gr/Re2) in their calculations, their prediction of frictional pressure-drop is significantly higher than the results obtained in this study. Figure 3 also suggests that the trend of the Yamashita et al. [14] correlation is different from both the other correlations and the current experimental results. The root mean square error (RMSE) of the plotted data in Figure 3 of the Blasius formula shows the least RMSE compared to other correlations for this data set.

The buoyancy effect in the horizontal supercritical flow causes stratification of the flow, where, the low density fluid occupies the upper part of the channel and the high density fluid flows near the lower surface. Moreover, free-convection due to buoyancy in the horizontal pipe induces a secondary flow with transverse circulation which increases the frictional pressure-drop.

Gr/Re^2 was reported in a few experimental pressure-drop studies. Ishigai et al. [15] reported that their data fell into Gr/Re^2<0.013-0.035, while for the Razimuvsky et al. [16] experimental data; the Gr/Re^2 was less than 0.003. In the present study the averaged Gr/Re^2 along the heated channel was between 0.1-0.8, which is significantly higher than the previous studies by Ishigai et al. [15] and Razimuvsky et al. [16]. Also, it was found from the present study that the frictional pressure-drop depends on the averaged value of Gr/Re^2. The "data sets" with lower mass flow-rates have larger values of Gr/Re^2 and consequently, larger frictional pressure-drops. All in all, the computed frictional pressure-drops for this study fall within 1-1.2% of the Blasius formula perdition for both cases with the least and the most effects of buoyancy and therefore Blasius formula is suggested for numerical modelling purposes.

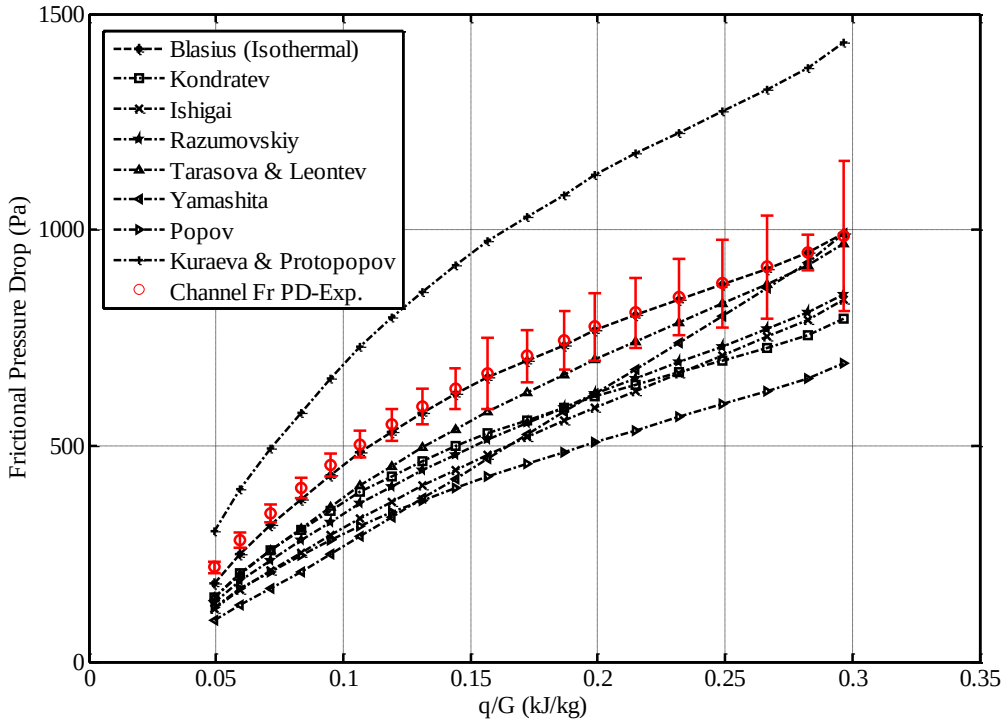

Figure 3 Comparison of frictional pressure drop between available correlations and present study for a data set

2.2 Steady-State parameters of the loop

In a natural circulation loop, mass flow-rate is a dependant variable and is a function of both the driving head, and the frictional and local pressure-drops in the loop (acceleration pressure-drop is zero for a closed loop). Figure 4(a)-(d) shows the variation of mass flow-rate for different working conditions. Figure 4(a) shows the effect of system pressure on the mass flow-rate in the natural circulation loop. It is evident from this figure that the mass flow-rate increases with increasing system pressure. Figure 4(b) shows the variation of flow-rate for different inlet temperatures of CO_2 flowing into the heated channel. The mass flow-rate for the case with lower temperature is higher which is due to the enhancement of driving head in the loop. Figure 4(c) illustrates the effect of outlet valve throttling on the mass flow-rate. In Figure 4(d) two data sets are compared in which the inlet K (local head loss coefficient) factor of one data set is approximately the same as the outlet K factor of the other data set. This example demonstrates the effect of equal inlet or outlet K factor on

the mass flow-rate in the natural circulation loop. Figure 4(d) shows that the outlet K factor reduces the mass flow-rate more significantly than the inlet K factor.

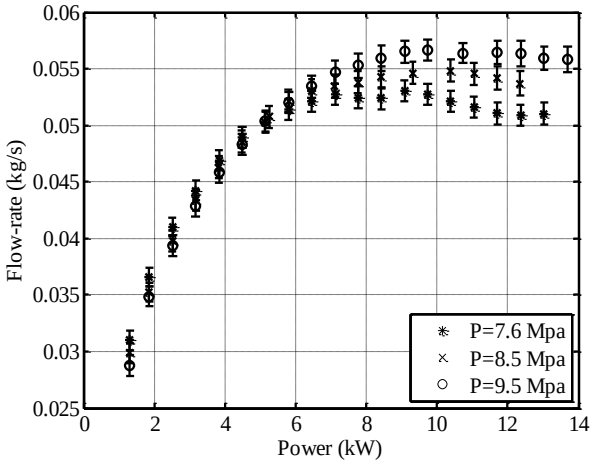

Figure 4(a) Variation of the mass flow-rate with power at different system pressures (T_{in}=25-26 ºC, K_{in}=0, K_{out}=0)

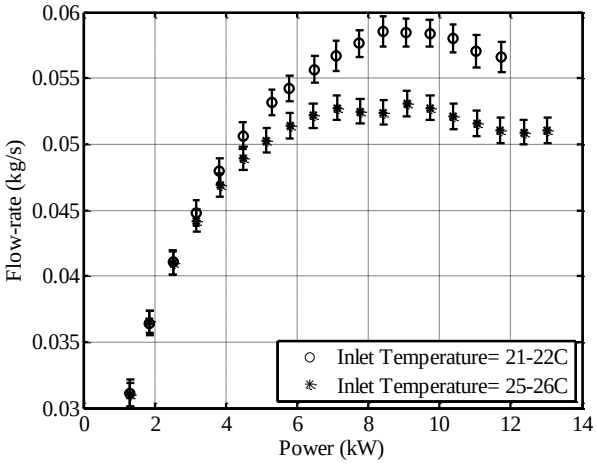

Figure 4(b) Variation of the mass flow-rate with power at different inlet temperatures (P_{system} =7.6 MPa, K_{in}=0, K_{out}=0)

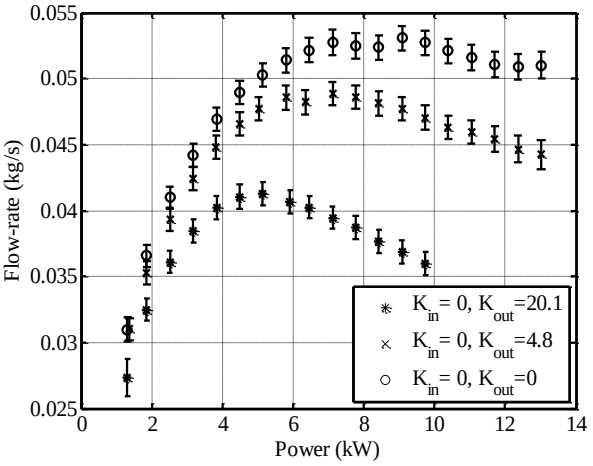

Figure 4(c) Variation of the mass flow-rate with power for different outlet K factors (P_{system}=7.6 MPa, Tin=25-26ºC, K_{in}=0)

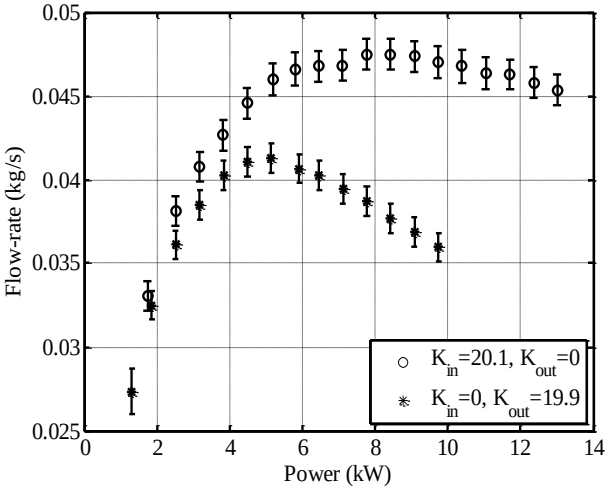

Figure 4(d) Variation of flow-rate with power for similar inlet/outlet K factors (P_{system} =7.6 MPa, T_{in}=25-26 ºC)

2.3 Flow oscillations result

A significant amount of time was spent on performing exploratory tests to locate the instability conditions for the present natural circulation loop. To achieve this purpose, some modifications were made on the experimental set-up.

Flow oscillations in this study were initiated following a perturbation in the mass flow-rate. Any change in the independent variables disturbs the velocity of CO_2 flowing into the heated channel. Most of the cases with flow oscillations were obtained occurred after increasing the heat flux on the heated channel, and oscillations of the flow were observed when the outlet temperature was higher

than the pseudo-critical temperature. In the present study, flow oscillations were observed in the negative slope part of the flow-rate versus power curve when the outlet temperature was above the pseudo-critical temperature. However, in the other experimental studies reported by other investigators, the temperature oscillations were observed when the outlet temperature was below but close to the pseudo-critical temperature. During flow oscillations, pressure-drop, wall surface temperature, and system pressure were oscillating in-phase or out of phase with the flow-rate.

To present the flow oscillations, the results of mass flow-rate are plotted versus time during a stepwise power increase for a data set. The flow oscillations and the effect of oscillations on the other measured parameters are discussed in the following for one case of flow oscillations. Figure 5 shows the variation of mass flow-rate with power increase. The trend of the increase and then decrease of mass flow-rate versus power is similar to the steady-state plots (Figure 4). Figure 6 shows inlet and outlet temperatures during a power increase for the same data set. The outlet temperature from the heated channel oscillated out of phase with the inlet flow-rate while the inlet temperature and heat flux on the heated channel were constant. The test illustrated in Figure 5 and 6 was performed at 8.00±0.02 MPa with an inlet temperature of 25-26 ºC when the outlet K factors for the pneumatic inlet and outlet valves were 0 and 20, respectively.

Flow instability emerged when the inlet velocity was disturbed at 9.63 kW. Diverging flow oscillations in this case led to diverging oscillations of the heated wall surface temperature as well, which reached 220 ºC at the location of TS 25B and the power was killed automatically (abrupt drop in power to zero in Figures 5 and 6). 220 ºC was the temperature limit for the heated channel for safe operation of the loop.

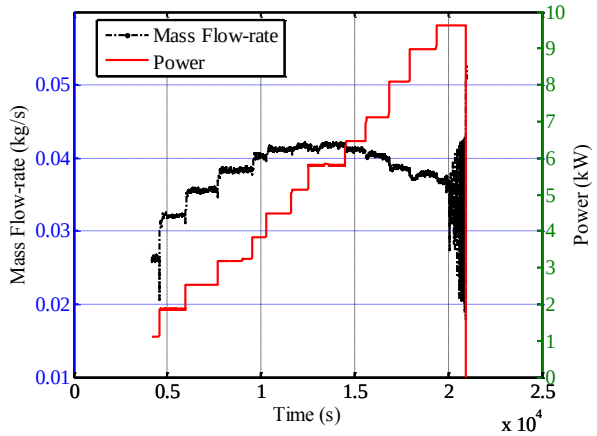

Figure 5 Evolution of flow-rate leading to the flow instability during power increase

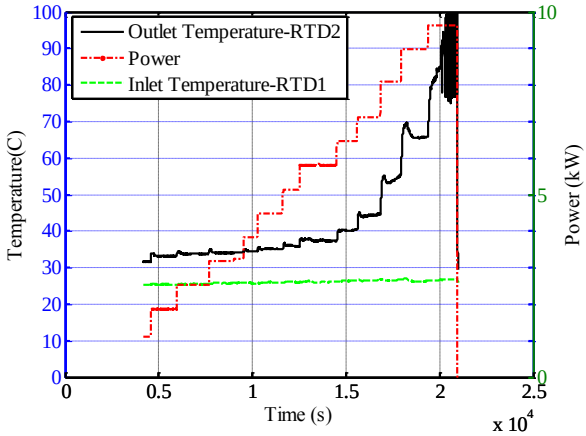

Figure 6 Variation of outlet temperature with power increase - constant inlet temperature

Flow instability started for this case when the outlet temperature was about 85 ºC (the pseudo-critical temperature of CO_2 at 8 MPa is ~34.6 ºC). However, the reading of outlet temperature was clipped for temperatures above 100 ºC due to the adjusted range of RTD2 transmitter. The peak to peak amplitude of the outlet temperature oscillations was 25ºC. The period of oscillation in this case was ~ 62-64s which was close to the transit time of the loop (~ 62s) for the steady-state conditions just before oscillations emerge.

Figure 7 shows the flow oscillation with more detailed information of different signals for a smaller period of time. Figure 7 (a) shows time trace of heat flux and flow-rate during flow oscillations. A second order Butterworth low pass filter with 0.02 Hz cut-off frequency was used for filtering the high frequency noise in the turbine flow-meter signal. Figure 5.25 (b) shows the oscillations of outlet temperature and flow-rate over time. It is evident from this plot that the outlet temperature oscillates out of phase with flow-rate, while the inlet temperature of CO_2 was constant (Figure 6).

When the fluid temperature is increased in a closed loop (constant volume), system pressure increases due to the fluid expansion. This trend was recorded during oscillations of the flow for a system pressure. Similar to the outlet temperature curve, system pressure oscillates out of phase with the inlet flow-rate (Figure 7 (c)). The maximum peak to peak amplitude of oscillations of system pressure in this case was approximately 0.1 MPa (100 kPa) for the last oscillation just before the power shutdown. The circled regions in Figure 7 (c) show the disturbances made to the flow by perturbing the system pressure. Figure 7 (d) shows the water flow-rate and temperature at the inlet of the heat exchanger in the secondary side. As shown in this plot both inlet temperature and flow-rate in the secondary side were constant during flow oscillations.

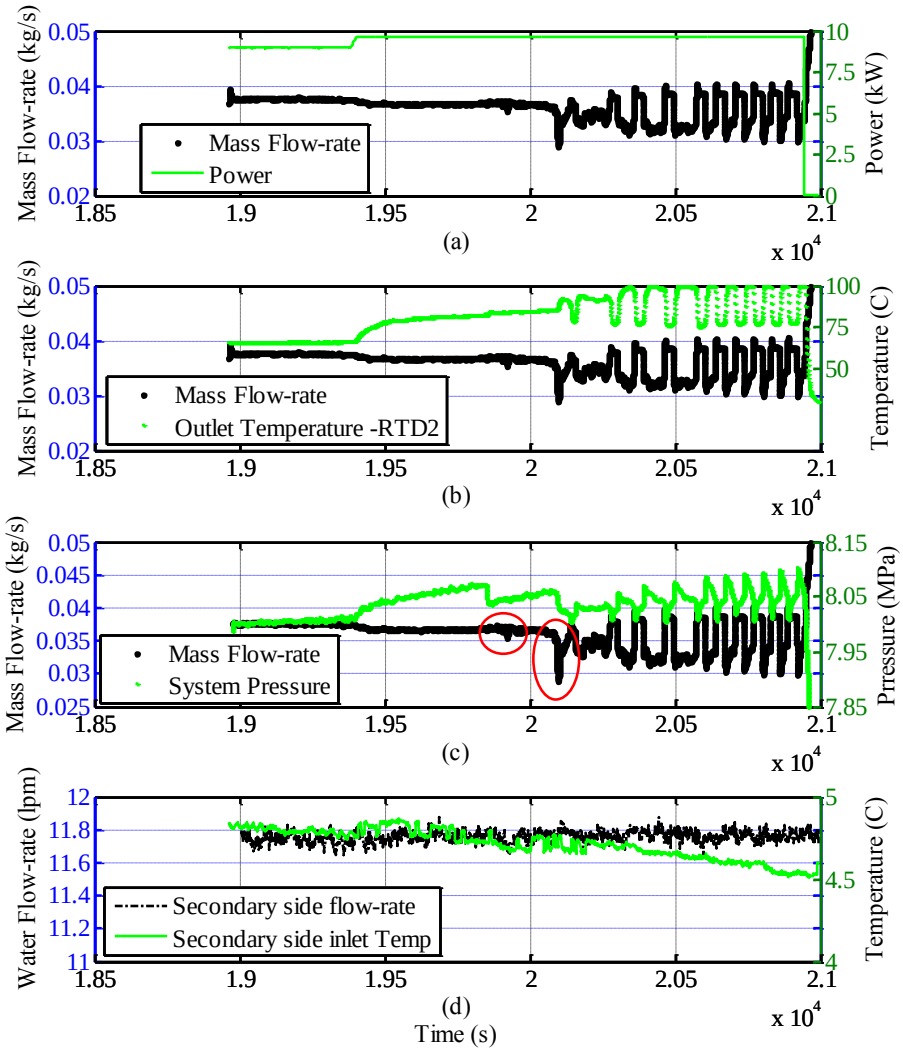

Figure 7 Detailed instability results for Case 1

3. Conclusion

From this experimental study it was concluded that available correlations used for approximating the frictional pressure-drop, underestimated the frictional pressure-drop obtained from this experimental study (except for Kuraeva & Protopopov and Blasius). Moreover, it was found that the buoyancy affects the frictional pressure-drop for the horizontal heated tube due to inducing a secondary flow. However, in the present experimental study, the frictional pressure-drop data fell within 1-1.2 of the Blasius formula. Therefore, among available correlations used for comparison, the Blasius correlation is suggested for use in numerical 1-dimensional modelling.

All cases with flow oscillations were observed on the negative slope part of the flow-rate versus power curve, which is similar to the second type of density wave oscillations in two-phase natural circulation loops. During flow oscillations, the heated wall surface temperature, system pressure, and outlet temperature were oscillating, while the power, inlet temperature, secondary side flow-rate, and water temperature were constant. Oscillations of outlet temperature and system pressure were out of phase with the oscillations of flow-rate. In all cases of flow oscillations, the outlet valve was partially closed. It worth noting that, flow oscillations were observed for the cases with an inlet temperature of 20-25ºC when the system pressure was 7.6-8.5 MPa. No flow oscillations were observed at 9.5 MPa in the experiments performed based on the test matrix.

4. References

[1] V. Chatoorgoon, "Stability of Supercritical fluid flow in single–channel natural convection loop", International Journal of Heat and Mass Transfer, Vol. 44, 2001, 1963-1972.

[2] V. Chatoorgoon, A. Voodi, D. Fraser, "The stability boundary for supercritical flow in natural convection loops. Part I. H2O studies", Nucl. Eng. Des., Vol. 235, 2005, 2570–2580.

[3] V. Chatoorgoon, A. Voodi, P. Upadhye, "The stability boundary for supercritical flow in natural convection loops. Part II. CO2 and H2", Nucl. Eng. Des., Vol. 235, 2005, 2581–2593.

[4] P. Jain and R. Uddin, "Steady state and numerical analyses of supercritical CO2 natural circulation loop", Proceedings of ICONE14-89103, Miami, Florida, USA, July 17-20.

[5] R. Jain, M. L. Corradini, "A linear stability analysis for natural-circulation loops under supercritical conditions", Nuclear Technology, Vol. 155, 2006, 312–323.

[6] S. Lomperski, D. Cho, R. Jain, M.L. Corradini, "Stability of a natural circulation loop with a fluid heated through the thermodynamic pseudocritical point", In: Proceedings of ICAPP'04, Pittsburgh, PA, USA, June 13–17 (Paper 4268).

[7] M. Sharma, P.K. Vijayana, D.S. Pilkhwala, Y. Asako,"Steady-state and stability characteristics of natural circulation loops, operating with carbon dioxide at supercritical pressures for open and closed loop boundary conditions" Nuclear Engineering and Design, Vol. 265, 2013, 737– 754.

[8] Y. Chen, M. Zhao, C. Yang, K. Bi, K. Du, "Experiment of heat transfer of supercritical water in natural circulation with different diameters of heated tubes", ISSCWR6-13097, ISSCWER-6 March 2013, Shenzhen, Guangdong, China.

[9] F. LV, Y.P. Huang, Y.L. Wang, X. Yan, "Experimental Observation of Supercritical Water Natural Circulation Instabilities", The 15th International Topical Meeting on Nuclear Reactor Thermalhydraulics, NURETH15-193, Pisa, Italy, May 12-15, 2013.

[10] J. Mahmoudi, "Experimental thermal-hydraulic study of a supercritical CO_2 natural circulation loop", M.Sc. thesis, University of Manitoba, 2014.

[11] R. J. Moffat, "Describing the uncertainties in experimental results", Experimental Thermal and Fluid Science, Vol. 1, Issue 1, 1988, Pages 3–17.

[12] I. L. Pioro, R.B. Duffey, T.J. Dumouchel, "Hydraulic resistance of fluids flowing in channels at supercritical pressures (survey)", Nuclear Engineering and Design, Vol. 23, 2004 187–197.

[13] I.V. Kuraeva, V.S. Protopopov, Mean friction coefficients for turbulent flow of a liquid at a supercritical pressure in horizontal circular tubes, High Temp. 12 (1) (1974) 194–196.

[14] T. Yamashita, H. Mori, S. Yoshida, M. Ohno,"Heat transfer and pressure-drop of a Supercritical pressure fluid flowing in a tube of small diameter", Memoirs of the Faculty of Engineering, Kyushu University, v 63, n 4, p 227-244, December 2003.

[15] S. Ishigai, M. Kadji, M. Nakamoto, "Heat transfer and pressure drop under water flow at supercritical pressure", JSME J. Ser. B 47 (424) (1981) 2333–2349.

[16] V.G. Razumovskii, A.P. Ornatskii, K.M. Maevskii, "Hydraulic resistance and heat transfer of smooth channels with turbulent flow of water of supercritical pressure", Thermal Eng. 31 (2) (1984) 109–113.

[17] I. E. Idelchik, "Handbook of hydraulic resistance", 2nd edn. Hemisphere, Washington (1993)

5. Appendix A

Table A1 Available friction-factors used in the comparison

Name	Formula
Blasius	f=0.184Re$^{-0.2}$
Kondrat'ev	f=0.188Re$^{-0.22}$
Ishigai	$\frac{f}{f_{iso}} = \left(\frac{\mu_b}{\mu_w}\right)^{-0.25}\left(\frac{\rho_b}{\rho_w}\right)^{-0.18}$
Razumovskiy	$\frac{f}{f_{iso}} = \left(\frac{\mu_w}{\mu_b}\frac{\rho_w}{\rho_b}\right)^{n}$
Tarasova & Leontev	$\frac{f}{f_{iso}} = \left(\frac{\mu_w}{\mu_b}\right)^{0.22}$
Yamashita	$\frac{f}{f_{iso}} = \left(\frac{\mu_w}{\mu_b}\right)^{0.72}$
Popov	$\frac{f}{f_{iso}} = \left(\frac{\rho_w}{\rho_b}\right)^{0.4}$
Kuraeva & Protopopov	$\frac{f}{f_{iso}} = \left(\frac{\mu_w}{\mu_b}\right)^{0.22} \times 2.15 \times \left(\frac{Gr}{Re^2}\right)^{0.1}$
f_{iso}= Filonenko	$f_{iso} = \frac{1}{\left(1.82 log_{10}^{Re_b} - 1.64\right)^2}$

* subscripts *b* and *w* corresponds to the bulk and near wall properties

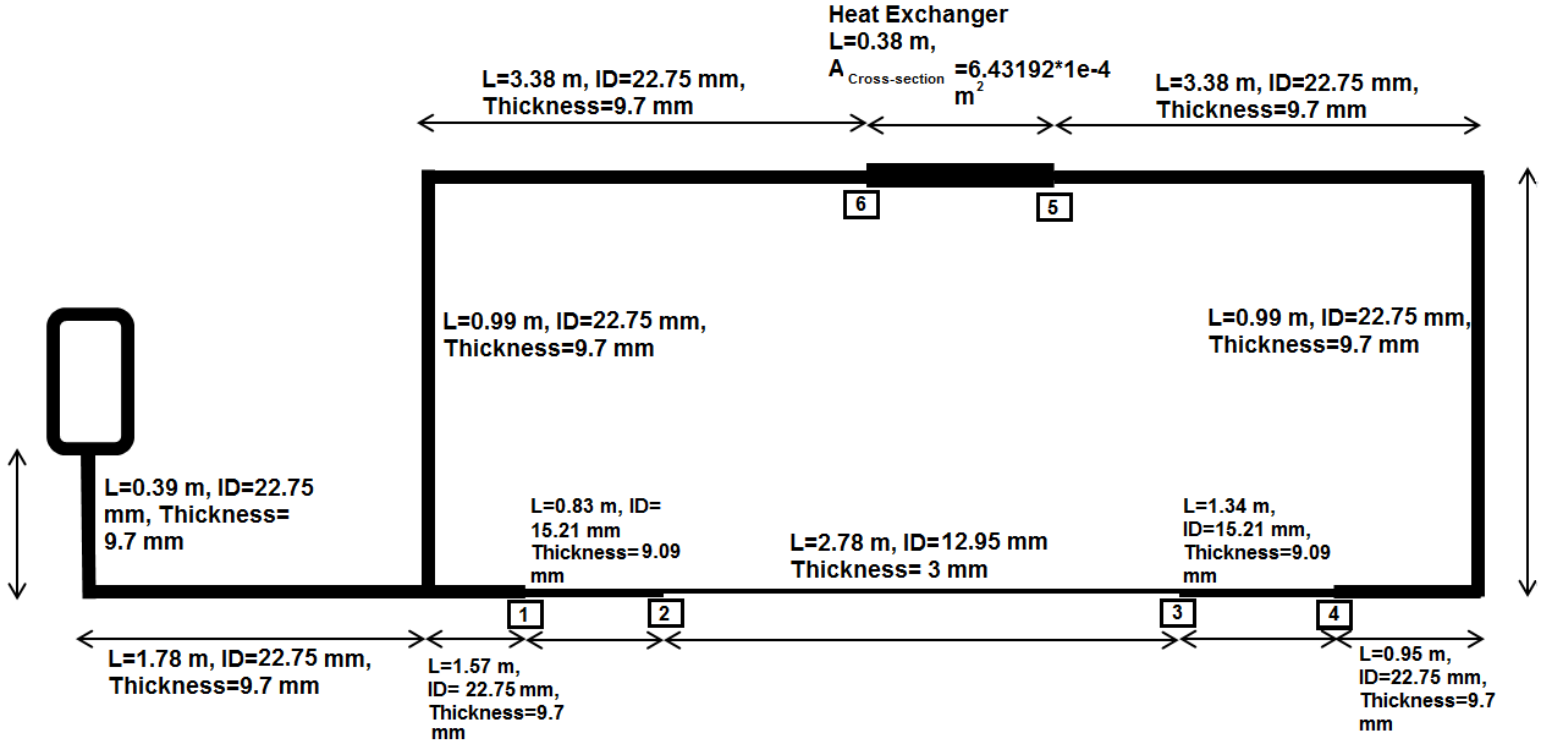

Figure A1Dimensions of the loop

Table A2 Calculated local K factors for area changes and elbows

Name	K_1	K_2	K_3	K_4	K_5	K_6	Elbows
K factor	0.07	0.18	0.1	0.3	2	2.7	2.16

* Calculated according to Idelchik [17]